Proceedings of the ASME 2011 30th International Conference on Ocean, Offshore and Arctic Engineering
OMAE2011
June 19-24, 2011, Rotterdam, The Netherlands

OMAE2011-49296

A FINITE ELEMENT STUDY OF MULTI-MODE VIV OF SLENDER RISER EXPERIENCING NON-UNIFORM FLOW

Li Min
School of Aeronautics Sciences and Engineering, Beijing University of Aeronautics and Astronautics
Beijing 100191, China

Chen Weimin
Key Laboratory of Environmental Mechanics, Institute of Mechanics, CAS
Beijing 100190, China

Zhang Liwu
Key Laboratory of Environmental Mechanics, Institute of Mechanics, CAS
Beijing 100190, China

ABSTRACT

The dynamic characteristics of deepwater riser usually present serried modes with lower frequencies, because structural flexibility is very large due to high aspect ratio (ratio of length to diameter of riser). Moreover, in practice flow velocity usually distributes non-uniformly along the riser length. A coupling model, for multi-mode VIV (vortex-induced vibration) of slender riser experiencing non-uniform flow, by means of finite element simulation combined with the hydrodynamic model taking account of the interaction between fluid and structure in time-domain, is proposed. VIV responses of slender risers respectively in uniform, stepped and shear flow are explored. Satisfied agreements with experiment results are observed. Additionally, based on the numerical simulations effects of reduced velocity and modal energy on modal weight are explored. We note that for case of multi-mode vibration the participating modes tend to distribute by groups..

KEYWORDS: deepwater riser; finite element simulation; vortex-induced vibration; multi-mode

1. INTRODUCTION

With the development of oil and gas exploration in deep sea, more and more deepwater platforms such as tension leg platforms, spar platforms, semi-submersible platforms have been put into service. The marine riser of these platforms is used to transport gas, oil and optical (or electrical) information. For a slender riser experiencing non-uniform flow, its wake fluid field, body motion and the interaction between fluid and structure are complex. For example, the vortex shedding mode and frequency vary along the riser length, or no longer keep constant. Moreover, the dynamic characteristics of slender riser usually present low-frequency and high-density natural modes due to large structural flexibility. Then the VIV of a slender riser experiencing non-uniform flow often presents new phenomena[1-6] such as multi-mode vibration , travelling wave and

 Copyright © 2011 by ASME

Downloaded 20 Sep 2012 to 141.213.173.17. Redistribution subject to ASME license or copyright; see http://www.asme.org/terms/Terms_Use.cfm

wide–band random vibration. Therefore, the prediction of VIV becomes more challenging.

In recent years large numbers of large-scale experiments and 3D CFD simulations were implemented[7-13]. The vortex mode and fluid force distribution for low Re number (10^2-10^3) were studied. Mechanism and empirical formula based on large-scale experiments were developed. Among these researches, the multi-mode vibration and drag coefficient by Huarte[6], high-mode lock-in by Vandiver[12] and modal weight by Huse[7] & Lie[13] provided fruitful bases for the prediction of multi-mode VIV.

In this study a numerical simulation model based on finite element method is developed for multi-mode VIV of slender riser. An coupling model of vortex-induced lift coefficient C_L, expressed by the instantaneous motion of structure, is proposed. This model can avoid costly computation of iteration calculation and is more suitable to time domain calculation by FEM code. At last, illustrative examples are given, in which the phenomena of multi-mode VIV such as the discrete modal weight and scattering mode distribution are explored for various flow fields, i.e. the uniform, stepped and shear flow.

2. HYDRODYNAMIC MODEL AND FINITE ELEMENT SIMULATION

2.1 Hydrodynamic Model

For a riser described as a tension Euler beam (shown in Fig. 1), the governing equation is:

$$m\frac{\partial^2 y(z,t)}{\partial t^2}+\gamma\frac{\partial y(z,t)}{\partial t}+EI\frac{\partial^4 y(z,t)}{\partial z^4}-T\frac{\partial^2 y(z,t)}{\partial z^2}=f(z,t) \qquad (1)$$

where $y(z,t)$ is the displacement of structure, m and γ are the mass and damping coefficient of unit length of beam; EI and T are the bending stiffness and axial tension. $f(z,t)$ is the hydrodynamic force consisting of vortex-induced lift force $f_v(z,t)$ and fluid drag force $f_f(z,t)$. Exact formula of hydrodynamic force and the solution of VIV are difficult to be directly derived because of the complicated interaction between fluid and structure.

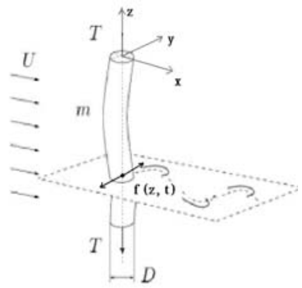

Figure 1 Sketch of a tension beam undergoing VIV

Here the hydrodynamic forces $f_v(z,t)$ and $f_f(z,t)$ are given respectively as follows:

$$f_v(x,t)=(1/2)C_L\rho V^2 D\sin\omega_v t \qquad (2a)$$

$$f_f(z,t)=\frac{1}{2}C_D\rho D(V-\dot{y})|V-\dot{y}|+C_A\frac{1}{4}\pi D^2\rho(\dot{V}-\ddot{y})+\frac{1}{4}\pi D^2\rho\dot{V} \qquad (2b)$$

where ρ and V are the density and velocity of fluid respectively, ω_v is the vortex shedding frequency (equal to the natural frequency of structure as lock-in occurring). C_L is the vortex-induced lift coefficient. C_D and C_A are the drag and added mass coefficients respectively, which can be determined by experiment.

Generally, C_L should be a function of variables related to structural motion so as to take account of the interaction between fluid and structural dynamics. Existing lift curve is presented as a hyperbolical curve of C_L against structural amplitude as shown in Fig.2[14], of which the coordinates of key points such as $C_{L\max}$, C_{LA0}, $\bar{A}_0$ and $\bar{A}_{L\max}$ are based on experimental results. However, for our problem the amplitude of structure is unknown before the calculation. And complex iteration is needed, which is computationally expensive. Moreover, the calculation including such iteration in dynamic response is difficult to implement in time domain using existing finite element code. Therefore, an alternative lift curve expressed by instantaneous motion of structure is proposed here.

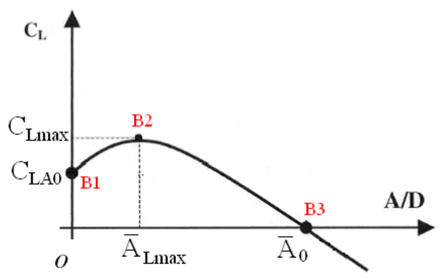

Figure 2 Lift curve

The alternative lift coefficient C_L assumed as a

Copyright © 2011 by ASME

Downloaded 20 Sep 2012 to 141.213.173.17. Redistribution subject to ASME license or copyright; see http://www.asme.org/terms/Terms_Use.cfm

function of structure motion velocity is required to make the lift force input the same value of energy to structure as the previous force in a motion period. The formula of C_L is written as

$$C_L(\dot{y}) = C_{L0} + a\dot{y} + b\dot{y}^2 + c\dot{y}^3 \tag{3}$$

where C_{L0} indicates the lift coefficient when the amplitude $A/D=0$. The structural motion in lock-in is assumed as $y = A\sin(\omega t)$, and the motion velocity is $\dot{y} = A\omega\cos(\omega t)$.

Then the energy input by the lift force $F_1 = F_0\cos(\omega t)$ where $F_0 = (1/2)C_{L0}\rho V^2 LD$, in a one-fourth period can be written as:

$$W_0 = \int_0^{\frac{T}{4}} F_0 A\omega(\cos\omega t)^2\,dt = \frac{\pi}{4}F_0 A \tag{4}$$

The energy input by the lift force

$$F = F_0\cos(\omega t) + a\dot{y} + b\dot{y}^2 + c\dot{y}^3 \tag{5}$$

is written as follows:

$$\begin{aligned} W_1 &= \int_0^{\frac{T}{4}} FA\omega(\cos\omega t)^2\,dt \\ &= \frac{\pi}{4}F_0A + a'A^2 + b'A^3 + c'A^4 \end{aligned} \tag{6a}$$

So we have

$$W_1/W_0 = 1 + a''A + b''A^2 + c''A^3 \tag{6b}$$

where $a'' = (\omega/F_0)a$, $b'' = (8\omega^2/3\pi F_0)b$ and $c'' = (3\omega^3/4F_0)c$. Therefore a new lift coefficient can be written as:

$$C''_L = C_{L0}(1 + a''A + b''A^2 + c''A^3) \tag{7}$$

where the values of a, b, c and C_{L0} can be resolved by making the new curve fit with the original curve at the key points, e.g. points B1, B2 and B3 in Fig.2. A group of equations describing the relationship between the existing curve and the new curve is as follows:

$$C_{L0} = C_{LA0}$$

$$C_{L0}[1 + \frac{\omega}{F_0}a\overline{A}_{L\max} + \frac{8\omega^2}{3\pi F_0}b(\overline{A}_{L\max})^2 + \frac{3\omega^3}{4F_0}c(\overline{A}_{L\max})^3] = C_{L\max}$$

$$\frac{\omega}{F_0}a + \frac{16\omega^2}{3\pi F_0}b\overline{A}_{L\max} + \frac{9\omega^3}{4F_0}c(\overline{A}_{L\max})^2 = 0$$

$$C''_L[1 + \frac{\omega}{F_0}a\overline{A}_0 + \frac{8\omega^2}{3\pi F_0}b(\overline{A}_0)^2 + \frac{3\omega^3}{4F_0}c(\overline{A}_0)^3] = 0$$

where $\overline{A}_0$ and $\overline{A}_{L\max}$ is the amplitudes when C_L=0 and $C_L = C_{L\max}$ respectively (as shown in Fig.2). Based on the presented lift model, finite element simulation can be carried out to obtain the dynamic response of a riser undergoing VIV.

2.2 Finite Element Simulations

Both the vortex-induced lift force $f_v(z,t)$ and the drag force $f_f(z,t)$ exerted by the ambient fluid are loaded along the riser length after the manners of distributing in the excitation region and damping region respectively. Then VIV response is calculated by finite element simulation.

To verify the proposed approach, the numerical results are compared experimental results (see Fig. 3), i.e. a rigid cylinder moving in a manner of single-mode vibration in uniform flow by Williamson(1999)[15] (Fig. 3a); and a flexible cylinder moving in a manner of multi-mode vibration in stepped flow by Chaplin(2005)[16] (Fig. 3c).

In our numerical simulations, the hydrodynamic coefficients are $C_A = 1.0$, $C_d = 1.2$; and the lift coefficients are $C_L = 0.5 + 1.82A - 1.29A^2 - 0.707A^3$ and $C_L = 0.22 + 1.62A - 2.31A^2 + 0.754A^3$ for cases of rigid and flexible cylinder respectively.

For case of rigid cylinder, the calculated amplitude ($A/D = 0.78$) is in a satisfied agreement with the experiment data ($A/D = 0.81$). And the response is characterized by a single-mode vibration. For the flexible cable, both single-mode vibration involving mode 3 only and multi-mode vibration involving mode 3 and 4 are carried out. Numerical results, plotted as rms displacement along riser length and temporal-spatial evolution, are shown in Fig. 3b and 3c respectively. It is seen that compared with the single-mode vibration, the multi-mode vibration agrees better with experimental results both on outer and inner envelopes of the rms curve. Additionally, travelling effect is observed in Fig.3c where multi-mode vibration occurs and no anti-node appears. Figure 3b implies that the single-mode vibration is dominated by a standing wave and apparent anti-nodes can be observed.

Copyright © 2011 by ASME

Downloaded 20 Sep 2012 to 141.213.173.17. Redistribution subject to ASME license or copyright; see http://www.asme.org/terms/Terms_Use.cfm

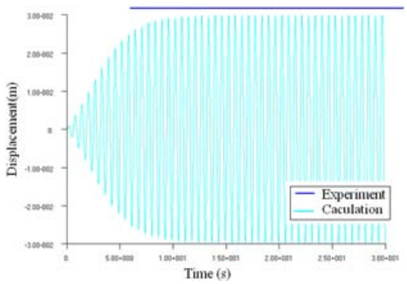

(a) Rigid cylinder vibrating in a manner of single-mode

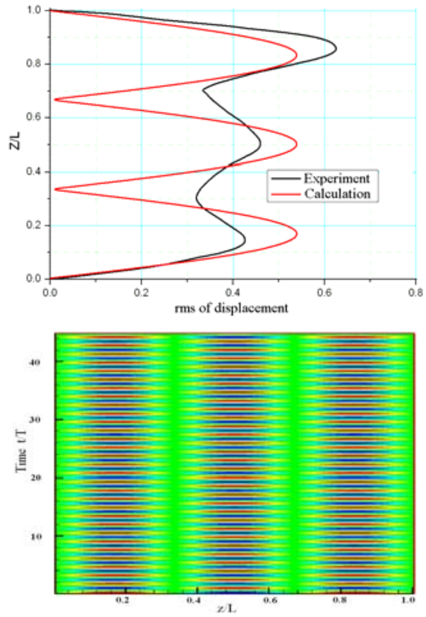

(b) Flexible cable vibrating in a manner of single-mode (mode 3)

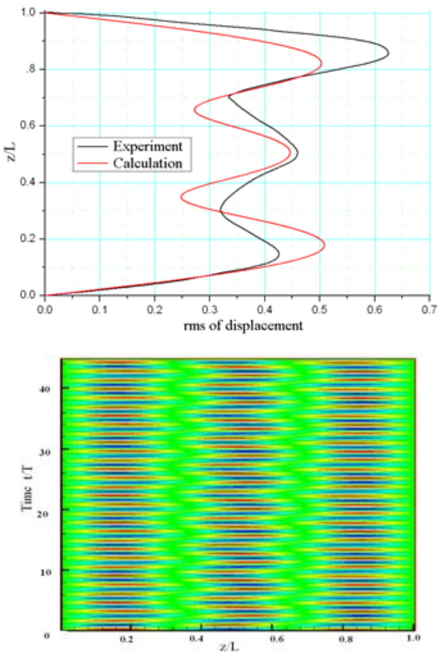

(c) Flexible cable vibrating in a manner of multi-mode (mode 3 and 4)

Figure 3 Comparisons between the presented numerical results and the existing experimental results of (a) rigid cylinder vibrating in a manner of single-mode; and (b) flexible cylinder vibrating in a manner of single-mode and (c) multi-mode.

3. MULTI-MODE VIV RESPONSE AND DISCUSSIONS

The multi-mode vibration in two fluid fields, i.e. a stepped flow and a linear shear flow, are examined and compared with experimental results. Additionally, for case of stepped flow, effects of reduced velocity on modal weight are explored. And for case of shear flow, the distribution of the participating modes is discussed.

3.1 VIV in stepped flow

For case of risers with large aspect ratio (more than 10^2), multi-mode vibration often occurs even in uniform flow. The determination of the length of modal excitation region is important to accurately predict VIV. Since the flow velocity non-uniformly distributes along the riser length, the problem of modal excitation length can be simplified into the weight of participating modes. A group of modal weights based on experiments by Chaplin[16] are listed in Table 1. Here we normalized the modal weight and plotted it against the reduced velocity ($V_r = V/Df_n$) in Fig.4.

Table 1 and Fig. 4 show that multiple modes, i.e. mode 4-8, participate the vibration. The dominating mode (with the largest value of modal weight) is not yet the highest mode as regarded in previous works[17,4]. It is noted that the mode, approximately corresponding 6~7 reduced velocity, tends to have a priority competing against other participating modes, or mostly become the dominating mode. A curve-fit function (see Fig.4) describing the relationship between the modal weight W_n and the reduced velocity V_r is proposed as follow:

$$W_n = \frac{1}{1.2} e^{(-e^{(-z_1)} - z_2 + 1)} \tag{8}$$

$z_1 = (V_r - 6.0)/0.7$, $z_2 = (V_r - 6.0)/1.6$

Figure 4 also indicates that the participating mode enters into lock-in region fast, or the curve is abrupt as V_r increasing from 4 to 7. And, it goes out of lock-in region slowly, or the curve becomes flat as V_r further increasing from 7 to 12.

The responses at different time steps are plotted and compared with the experimental results in Fig.5. Both numerical and experimental results indicate that the vibration is characterized by node-moving due to an

Copyright © 2011 by ASME

Downloaded 20 Sep 2012 to 141.213.173.17. Redistribution subject to ASME license or copyright; see http://www.asme.org/terms/Terms_Use.cfm

effect of travelling wave. Apparently, mode 4 dominates the vibration and the largest amplitude is up to 1.0.

Table 1 Experimental measurements of modal weight for cases of top tension of T=1073N and T=939N respectively

Mode number	Modal weight T=1073N	Modal weight T=939N
4	0. 08	0.01
5	0.12	0.15
6	0. 5	0.25
7	0.28	0.42
8	0.01	0.05

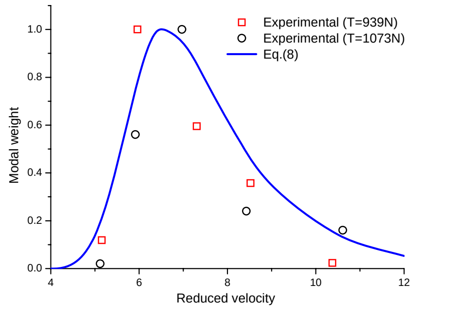

Figure 4 Effect of reduced velocity on the modal weight

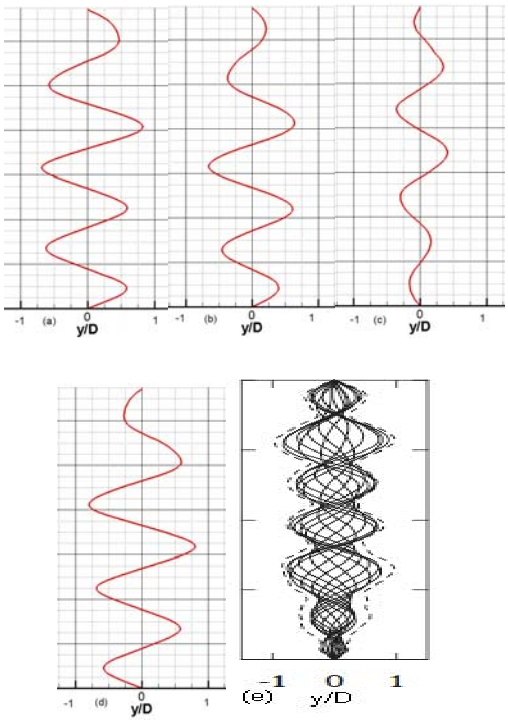

Figure 5 VIV amplitude of flexible riser experiencing stepped flow by numerical simulation (the four plots at different time step) and experiment (the last one by Chaplin(2005))

3.2 VIV in shear flow

In practice, many fluid fields such as ocean current and flow induced by internal-wave can be treated as shear flow. Multi-mode VIV in shear flow will be simulated and compared with the large-scale test (shown in Fig.6) by Trim(2005)[18]. Further, the distribution of participating modes will be explored. The VIV at ten different towing speeds were simulated. Here only the results of two towing speeds, i.e. 0.54m/s and 1.14m/s, are presented.

The modal excitation length l_n is proportional to the modal energy in a form of

$$l_n/l_m = P_n/P_m \tag{9}$$

The modal energy is written as[2,12]

$$P_n = (F_n)^2/(2R_n) \tag{10}$$

where modal force $F_n = \int_{L_n}(1/2)C_L\rho V(z)^2 D\varphi_n^2(z)dz$ and modal damping $R_{hn} = \int_{L-L_n} r_h(z)\varphi_n^2(z)\omega_n dz$. $\varphi_n(z)$ is the mode shape of mode n. It is noted that the potentially excitation regions distribute proportionally, not yet the regions of lower mode is overlapped by the regions of higher modes as required by the rule of the high mode priority[4,17].

The rms of displacement along the riser length calculated by both previous and presented method, i.e. by the rule of high mode priority and modal energy respectively, are shown in Fig. 7. Compared with the previous method, the presented model can predict a displacement response agreeing better with the experimental curve. It is also noted that the calculated vibration in Fig. 7b closes to the experimental result among the excitation region ($z/L = 0.0-0.4$), but becomes larger than the experimental results as approaching to the bottom end of riser. Or the calculated vibration keeps almost the same level along overall riser length, whereas the experimental vibration attenuates as approaching to the bottom end of riser due to an effect of travelling wave.

The dominating mode given by the presented model is also consistent with the experimental result. For example, Fig. 7a (0.54m/s towing speed) indicates that the dominating modes of both the presented model and experiment are mode 11. However, using the previous model, mode 14 is the dominating mode.

The modal excitation lengths of all participating modes are presented in Fig. 8 and compared with that by

Copyright © 2011 by ASME

Downloaded 20 Sep 2012 to 141.213.173.17. Redistribution subject to ASME license or copyright; see http://www.asme.org/terms/Terms_Use.cfm

the previous model. It is seen that the modal excitation length not yet averagely distribute as required by previous model. Taking case of 0.54m/s towing speed as an example (Fig. 8a), there are approximately 3 groups of participating modes, i.e. mode 6, mode 11&10 and mode 14. But by the previous model, all potentially participating modes have approximately same level of excitation power. Subsequently, it is difficult to exclude the modes whose vibration is in fact very weak.

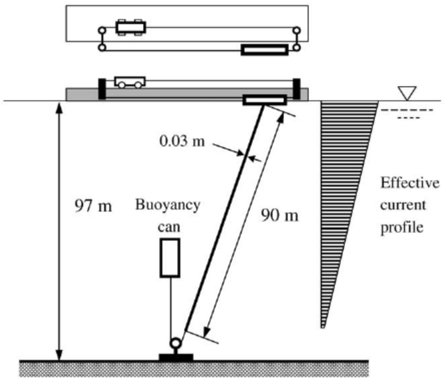

Figure 6 Experiment of flexible riser experiencing shear flow by Lie(1997)

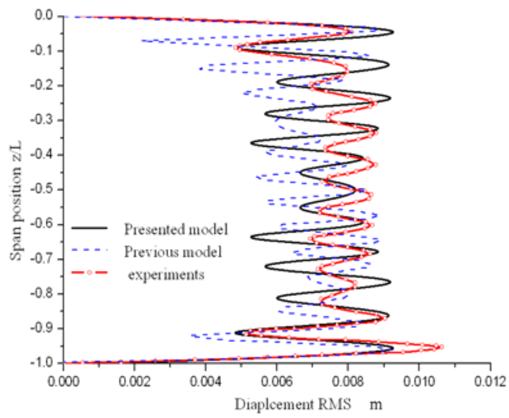

(a) 0.54m/s towing speed

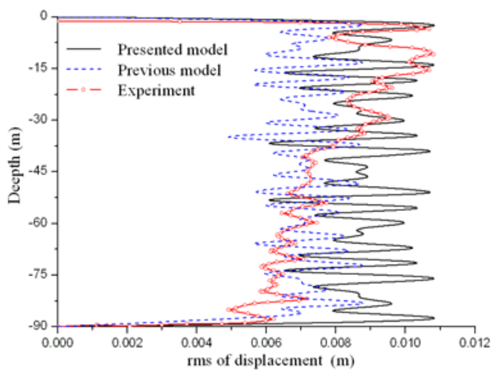

(b) 1.14m/s towing speed

Figure 7 Rms of displacement of flexible riser

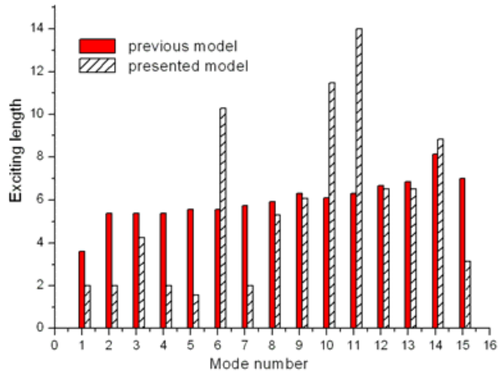

(a) 0.54m/s towing speed

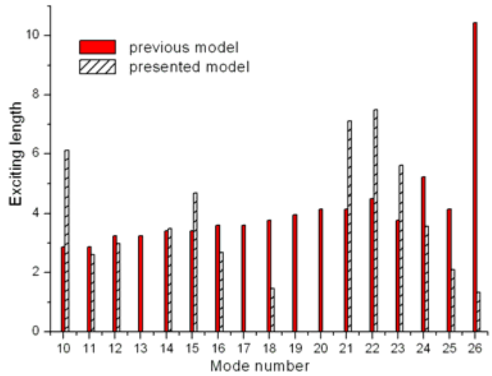

(b) 1.14m/s towing speed

Figure 8 Distribution of participating modes

4. CONCLUSIONS

A prediction approach for VIV of deepwater risers, using finite element simulation combined with a semi-empirical coupling hydrodynamic model, i.e. a time-domain analysis approach is proposed. VIV responses of a rigid cylinder elastically constrained in uniform flow, a slender risers respectively in stepped and shear flow are explored. Satisfied agreements with experiment results are observed. Based on our numerical results, we draw following conclusions:

(1) For multi-mode VIV in uniform or stepped flow, modal excitation region is sensitive to reduced velocity. A semi-empirical formula describing the relationship between the length of excitation region and reduced velocity is given.

(2) For multi-mode VIV in shear flow, modal excitation region is sensitive to modal energy, and the participating modes approximately distribute after a manner of scattering groups.

ACKNOWLEDGMENTS

This work is supported by the National Natural Science Foundation of China (Grant No. 10772183) and

Copyright © 2011 by ASME

Downloaded 20 Sep 2012 to 141.213.173.17. Redistribution subject to ASME license or copyright; see http://www.asme.org/terms/Terms_Use.cfm

The Intellectual Innovation Project of the Chinese Academy of Sciences (Grant No. KJCX2-YW-L07).

5. REFERENCE

[1] Sarpkaya, T., 2004. A Critical review of the intrinsic nature of vortex-induced vibration. Journal of Fluids and Structures Mechanics 46, 389-447.

[2] J.K.Vandiver, 1993, Dimensionless parameters important to the prediction of vortex-induced vibration of long, flexible cylinders in ocean currents , Journal of Fluids and Structures, 7(5):423-455.

[3] G. Moe, O. ARNTSEN, 2001, VIV analysis of risers by complex modes, in: 11th International Offshore and Polar Engineering Conference, 3: 426-430.

[4] Lyons G J, Patel MH. 1986, A prediction technique for vortex induced transverse response of marine risers and tethers. Journal of Sound and Vibration, 111(3): 467-487.

[5] Facchinetti, 2004, Vortex-induced traveling waves along a cable, European J. of Mech. B/Fluids, 16:199-208.

[6] Huera Huarte F J, Bearman P W, Chaplin J R, 2006, On the force distribution along the axis of a flexible circular cylinder undergoing multi-mode vortex-induced vibrations, Journal of Fluids and Structures 22: 897—903.

[7] Huse E, Kleiven G, Nielsen F G, Large scale model testing of deep sea risers, Proceedings of the Offshore Technology Conference, Houston, Texas, 1998, OTC 8701.

[8] Huse E, Kleiven G, Nielsen F G, VIV-induced axial vibration on deep sea risers, Proceedings of the Offshore Technology Conference, Houston, Texas, 1999, OTC 10932.

[9] Grant R., Litton R., Finn, L., Maher J., Lambrakos K., Highly Compliant Rigid Risers: Field Test Benchmarking a Time Domain VIV Algorithm, OTC 11995, 2000.

[10] Dong S, Karniadakis G E. 2005, DNS of flow past a stationary and oscillating cylinder at Re=10000. Journal of Fluids and Structures, 20: 519-531

[11] Yamamoto C T, Meneghini J R, Saltara F. 2004, Numerical simulations of vortex-induced vibration on flexible cylinders. Journal of Fluids and Structures, 19: 467-489.

[12] Vandiver J K. 2002, A Universal Reduced Damping Parameter for Prediction of Vortex-Induced Vibration, OMAE 2002, Oslo, Norway.

[13] Lie H, Kaasen H K, 2006, Model analysis of measurements from a large-scale VIV model test of a riser in linearly sheared flow, Journal of Fluid and Structures; 22: 557—575.

[14] Larsen, C.M., Vikestad, K., Yttervik, R. and Passano, E.: 2001, Empirical model for analysis of vortex induced vibrations - theoretical background and case studies, OMAE2001/OFT-1203, Rio de Janeiro June 2001.

[15] Khalak A.& Williamson C.H.K.. 1999, Motions, forces and mode transitions in vortex-induced vibrations at low mass-damping. Journal of Fluids and Structures, 13: 813-851.

[16] Chaplin J.R., P.W. Bearman, F.J. Huera Huarte, R.J. Pattenden. 2005, Laboratory measurements of vortex-induced vibrations of a vertical tension riser in a stepped current. Journal of Fluids and Structures, 21: 3–24.

[17] Chen WM, Zhang LW, Li M, 2009, Prediction of vortex-induced vibration of flexible riser using an improved wake-oscillator model. OMAE2009-79336, May 2009, Honolulu, Hawaii.

[18] Trim, A.D., Braaten, H., Lie H. et. 2005, Experimental investigation of vortex-induced vibration of long marine risers. Journal of Fluids and Structures, 21: 335–361.

Copyright © 2011 by ASME

Downloaded 20 Sep 2012 to 141.213.173.17. Redistribution subject to ASME license or copyright; see http://www.asme.org/terms/Terms_Use.cfm